Dynamic crack arrest capability of some metallic alloys and polymers

Gunasilan Manar[1,2], *Norazrina* Mat Jali[1,2], *Patrice* Longère[1,*]

[1]Université de Toulouse, ISAE-SUPAERO, Institut Clément Ader (CNRS 5312), Toulouse, France
[2]National Defense University of Malaysia, Kuala Lumpur, Malaysia

Abstract. We are here interested in the crack arrest capability under impact loading of metals and polymers used as structural and/or protection materials in aerospace engineering. Kalthoff and Winkler-type impact tests are carried out to that purpose on high strength AA7175 aluminum alloy and shock resistant polymethyl methacrylate (PMMA). Impact tests are carried out at impact velocities ranging from 50 m/s to 250 m/s and high speed camera is used to record the different steps of the failure process. For AA7175, early Mode II shear failure followed by late Mode I opening failure are seen. The premature ductile failure of the alloy is shown to result from a preceding stage of dynamic localization in the form of adiabatic shear bands. Impact tests on shock-resistant PMMA evidence the brittle feature of the material failure. It is notably shown that the higher the impact velocity (in the range 50-100 m/s) the larger the number of fragments. Moreover, depending on the impact velocity, changes in the crack path and thus in the mechanisms controlling the PMMA dynamic fracture can be seen.

1 Introduction

The investigation of the failure mechanisms occurring under high strain rate loading in engineering materials is a key point for the design of structures submitted to accidental overloads, as e.g. bird strike or fragment impact in the aerospace sector. In this context, we are here interested in the crack arrest capability under impact loading of metals and polymers used as structural and/or protection materials. In the philosophy of the crack arrest capability considered in the present work (not to be confused with the one of the crack arrest standard defined by ASTM E1221-96 for brittle fracture), an engineering structure is supposed to be initially weakened by a crack, resulting from e.g. fatigue loading, and the goal consists in determining the response of this pre-cracked structure to a high rate reloading. Kalthoff and Winkler (KW)-type impact tests were performed to that purpose.

The materials under consideration in the present work are high strength aluminum alloy (AA) on the one hand and shock resistant polymethyl methacrylate (PMMA) on the other hand.

Kalthoff and Winkler (KW)-type impact tests, see [1] and [2], which consist in impacting the edge of a double-notched plate were carried out using Institut Clément Ader Lab., STIMPACT impact facility (3 gas launchers with complementary performances), see Fig.1, at different impact velocities comprised between 50 and 250 m/s. The plate dimension was 40x82x6 mm^3 with notches of 300 µm-thickness and 20 mm-length. The double notched plate is placed inside a closed chamber as can be seen in Fig.2. The 6 m-length gas launcher was used to launch a 20mm-diameter cylindrical steel projectile. A Photron SA5 high speed camera was used to record the projectile/plate interaction at 10^5 fps (frame per second) and 320x192 $pixel^2$ spatial resolution.

Fig. 1. STIMPACT platform. Partial view of the gas launchers.

In parallel, quasi static tests were performed using standard tension-compression testing machines and high strain rate tests employing split Hopkinson pressure bar (SHPB) apparatus.

* Corresponding author: patrice.longere@isae.fr

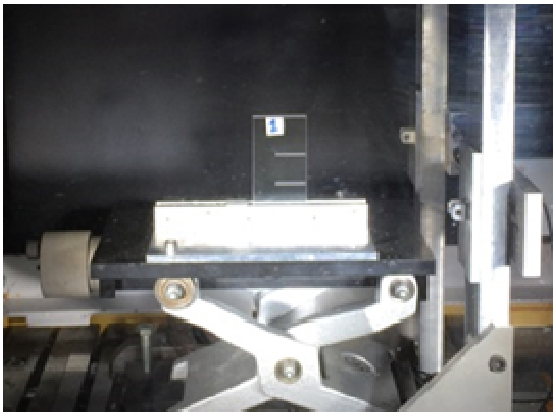

Fig. 2. View of the double notched plate (in PMMA) with the support table. The projectile hits the edge of the plate from the right side.

2 AA7175 aluminum alloy

The lightweight alloy under consideration is the Al-Zn-Mg AA7175 aluminum alloy provided in the form of plate in the T7351 metallurgical state for aircraft application.

2.1 Thermomechanical characterization

Fig.3 shows the temperature effect on AA7175 flow stress at low strain rate. The flow stress as well as strain hardening gradually decreases with increasing temperature. At 150° C there is only low strain hardening and at 200° C no hardening at all. Fig.4 shows the superposition of stress-strain curves at different strain rates during compression loading. As depicted in the figure, there is a sudden drop in stress at high strain rate for this alloy.

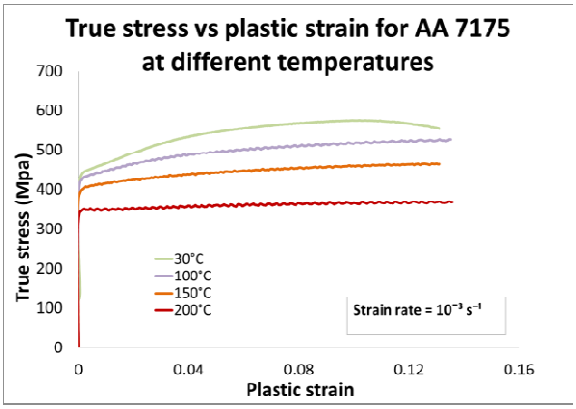

Fig. 3. Flow stress vs. plastic strain at various temperatures. AA7175. (tension).

Fig 5 shows the specimen after dynamic compression loading at a strain rate of 2020 s^{-1}. AA7175 specimen exhibits a cross shape band evidencing shear localization at high strain rate loading, see also [3]. The presence of these adiabatic shear bands (ASB) explains the premature failure of the specimen made of AA7175 featured by the drop in stress observed on the stress-strain curve in Fig.4 for strain rate of 2020 s^{-1}.

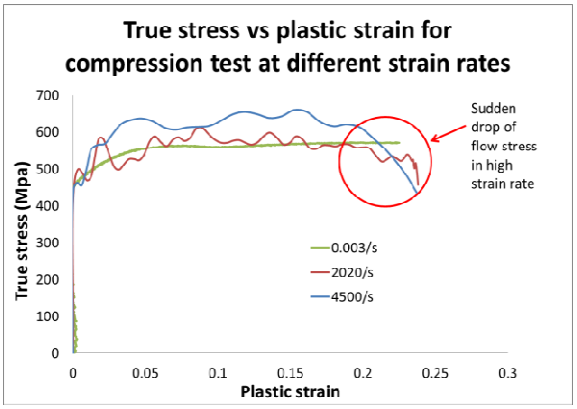

Fig. 4. Flow stress vs. plastic strain at various strain rates. AA7175 (Compression).

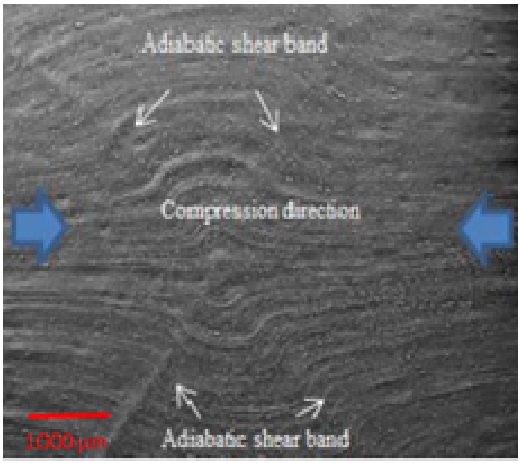

Fig. 5. Microstructural view of the post-mortem specimen after compression loading at 2020 s^{-1}.

2.2 Impact tests

Various KW-type impact test tests were performed at different impact velocities ranging from 100 m/s to 230 m/s. From 120 m/s, early Mode II shear ductile failure followed by late Mode I opening failure are seen for all tests. The complete failure of the plate, i.e. separation of the plate in different parts, is seen from 130 m/s. The post-mortem double-notched plate after impact at 120m/s (involving partial failure) is shown in Fig.6. The propagation of the crack in the same direction as the notch evidences the shear-controlled nature of the failure mode [4].

Fig.7 shows three images of the microstructure inside the crack zone at three different locations, see Fig.6. The initiation of the crack from the notch tip is characterized by flat shear evidencing shearing induced mode II failure, see image 3. According to image 2, crack propagation seems to proceed from predominant shearing induced Mode II (flat shear surface). Image 1 shows a bifurcation of the crack direction. Further analysis of the microstructure in this zone shows flat shear surface where mode II induced shear failure is dominant, see image 1. The observation of the crack lips

on higher impact velocity reveals the presence of ASB (not shown here).

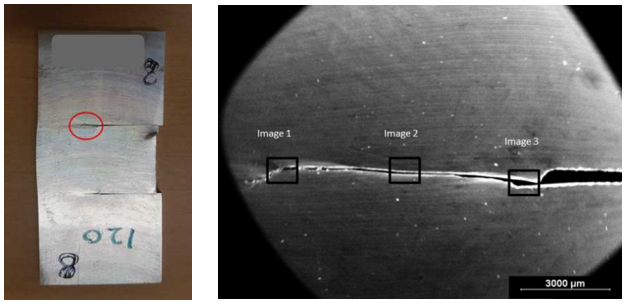

Fig. 6. Post-impacted double-notched plate. 120 m/s. Partial failure under Mode II shear-controlled crack propagation.

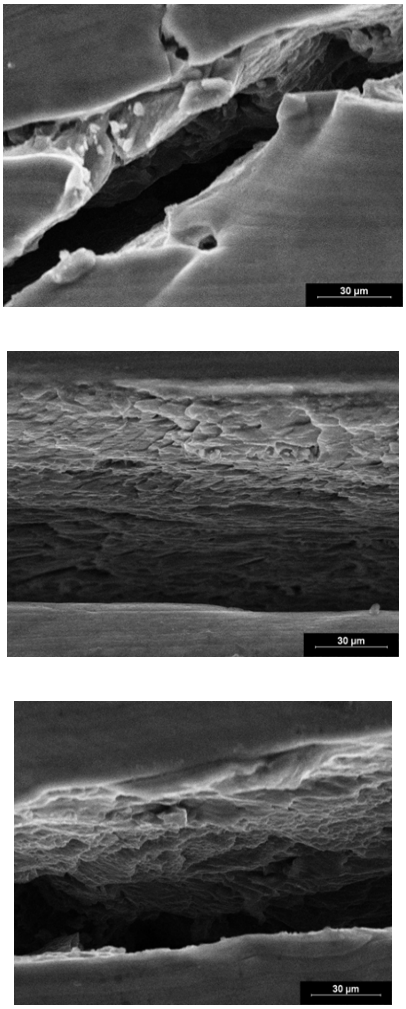

Fig. 7. Microstructure of post-impacted double-notched plate at 120 m/s. Top: Image 1. Middle: Image 2. Bottom: Image 3. See Fig.6.

2.3 Discussion

We are here defining the critical impact velocity for crack arrest (for the double-notched plates used herein) as the velocity above which the plate separates in different parts. The critical impact velocity for AA7175 is shown to be close to 130 m/s. Impact tests carried out on AA2024 alloys (not presented here) have evidenced a critical impact velocity close to 150 m/s. The less dynamic toughness of AA7175 can be explained by the formation of adiabatic shear banding. The latter is indeed known to result from thermomechanical instability and to make the failure premature.

3 Shock resistant PMMA

The shock resistant, highly transparent PMMA under consideration is the Plexiglass Resist® provided in the form of plate. It consists essentially of polymethyl methacrylate and a tough phase distributed therein which is usually present as a core/shell dispersion.

3.1 Thermomechanical characterization

Fig. 8 shows the flow stress vs plastic strain for Plexiglass Resist® under low strain rate tension and compression loading. The curves obtained are typical of the behaviour of polymers below glass transition, see [5-7] . The tension-compression asymmetry is significant for the PMMA under consideration, as well as the stress whitening effect under predominant tension loading.

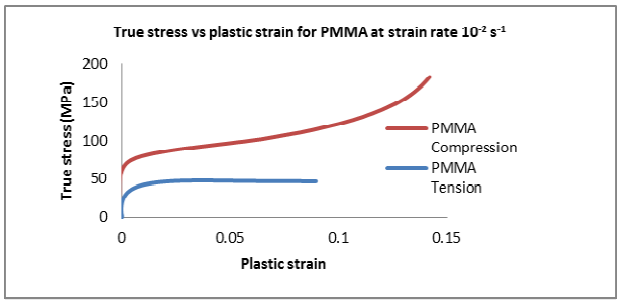

Fig. 8. Flow stress vs. plastic strain under compression and tension loading.

Plexiglass Resist® specimens after low and high strain rate compression loading are shown in Fig. 9. According to the latter, a complex pattern of strain localization bands can be seen inside dynamically deformed specimens.

Fig. 9. Specimens after compression loading. Left: low strain rate. Right: high strain rate. Plexiglass Resist®.

3.2 Impact tests

KW-type impact test were carried out at different impact velocities ranging from 50m/s to 80m/s. A frame of the interaction between the projectile and the double notched plate is shown in Fig.10. According to the latter, cracks

propagate symmetrically from the notch tips with a high angle, which is typical of a brittle fracture.

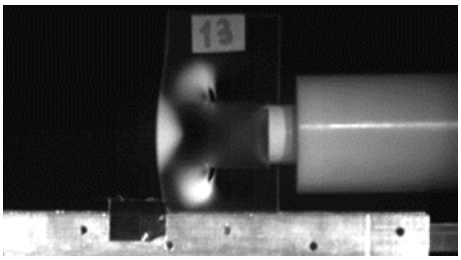

Fig. 10. Frame of the double notched plate/projectile interaction.

Fig.11 shows double notched plates after impact loading at 50m /s and 80 /s. According to Fig.11 and to other tests not presented here, it can be seen that the higher the impact velocity the larger the number of fragments.

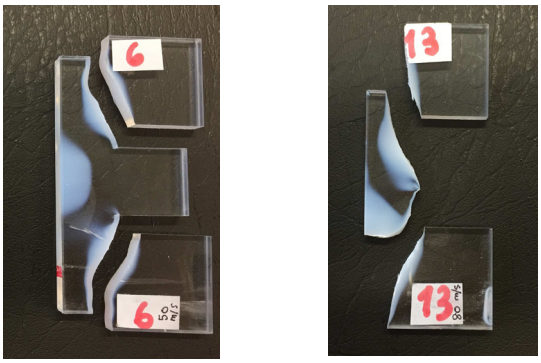

Fig. 11. Double notched plates after impact loading at 50m/s (left) and 80 m/s (right).

3.3 Discussion

The failure of the shock resistant PMMA under consideration, namely Plexiglass Resist®, is seen to be brittle. The number of fragments increases with increasing impact velocity. The cracks propagate inside wide zones of stress whitening. This stress whitened appearance is similar to the work in [8].

4 Concluding remarks

KW type impact tests performed in the present study show that the failure is ductile for high strength AA7175 aluminum alloy and brittle for shock resistant Plexiglass Resist® PMMA.

AA7175 shear-controlled failure under impact loading is made premature by the formation of adiabatic shear bands. The latter must accordingly be taken into account in the design of structures submitted to accidental events involving high strain rate loading.

Plexiglass Resist® tension-controlled failure under impact loading is seen to process inside wide zones of stress whitening. As for ASB in AA7175, the consequences of these wide zones should be accounted for in engineering design.

References

1. J.F. Kalthoff, S.Winkler, Failure mode transition of high rates of shear loading, in :C.Y. Chiem, H,-D. Kunze, L.W. Meyer (Eds), *Proceedings of the International Conference on Impact Loading and Dynamic Behavior of Materials*, Deutsche Gesellschaft fur Metallkunde, DGM-Verlag, Oberursel, Germany, pp. 185-195, (1987)
2. E. Roux, P. Longère, O. Cherrier, T. Millot, D. Capdeville, and J. Petit, "Analysis of ASB assisted failure in a high strength steel under high loading rate," *Mater. Des.*, vol. **75**, pp. 149–159 (2015)
3. D. H. Li, Y. Yang, T. Xu, H. G. Zheng, Q. S. Zhu, and Q. M. Zhang, "Observation of the microstructure in the adiabatic shear band of 7075 aluminum alloy," *Mater. Sci. Eng. A*, vol. **527**, no. 15, pp. 3529–3535 (2010)
4. P. Longere and A. Dragon, "Dynamic vs. quasi-static shear failure of high strength metallic alloys: Experimental issues," *Mech. Mater.*, vol. **80**, no. PB, pp. 203–218 (2015)
5. J. Richeton and S. Ahzi, "Influence of temperature and strain rate on the mechanical behavior of three amorphous polymers : Characterization and modeling of the compressive yield stress," vol. **43**, pp. 2318–2335 (2006)
6. W. Chen, F. Lu, and M. Cheng, "Tension and compression tests of two polymers under quasi- static and dynamic loading," vol. **21**, pp. 113–121, (2002)
7. E. M. Arruda, M. C. Boyce, and R. Jayachandran, "Effects of strain rate , temperature and thermomechanical coupling on the finite strain deformation of glassy polymers," vol. **19**, pp. 193–212 (1995)
8. L. Lalande, C. J. G. Plummer, P. Ge, and J. E. Ma, "Microdeformation mechanisms in rubber toughened PMMA and PMMA-based copolymers," vol. **73**, pp. 2413–2426 (2006)